Overexpression of mitochondrial GPAT in rat hepatocytes leads to decreased fatty acid oxidation and increased glycerolipid biosynthesis

Daniel Lindén,*,† Lena William-Olsson,* Magdalena Rhedin,* Anna-Karin Asztély,* John C. Clapham,* and Sandra Schreyer[1],*

AstraZeneca R&D,* Mölndal, Sweden; and Wallenberg Laboratory for Cardiovascular Research,† Göteborg University, Sweden

Abstract **Glycerol-3-phosphate acyltransferase (GPAT) catalyses the first committed step in glycerolipid biosynthesis. The mitochondrial isoform (mtGPAT) is mainly expressed in liver, where it is highly regulated, indicating that mtGPAT may have a unique role in hepatic fatty acid metabolism. Because both mtGPAT and carnitine palmitoyl transferase-1 are located on the outer mitochondrial membrane, we hypothesized that mtGPAT directs fatty acyl-CoA away from β-oxidation and toward glycerolipid synthesis. Adenoviral-mediated overexpression of murine mtGPAT in primary cultures of rat hepatocytes increased mtGPAT activity 2.7-fold with no compensatory effect on microsomal GPAT activity. MtGPAT overexpression resulted in a dramatic 80% reduction in fatty acid oxidation and a significant increase in hepatic diacylglycerol and phospholipid biosynthesis. Following lipid loading of the cells, intracellular triacylglycerol biosynthesis was also induced by mtGPAT overexpression. Changing an invariant aspartic acid residue to a glycine [D235G] in mtGPAT resulted in an inactive enzyme, which helps define the active site required for mammalian mtGPAT function. To determine if obesity increases hepatic mtGPAT activity, two models of rodent obesity were examined and shown to have >2-fold increased enzyme activity. Overall, these results support the concept that increased hepatic mtGPAT activity associated with obesity positively contributes to lipid disorders by reducing oxidative processes and promoting de novo glycerolipid synthesis.**—Lindén, D., L. William-Olsson, M. Rhedin, A-K. Asztély, J. C. Clapham, and S. Schreyer. **Overexpression of mitochondrial GPAT in rat hepatocytes leads to decreased fatty acid oxidation and increased glycerolipid biosynthesis.** ***J. Lipid Res.*** **2004.** 45: **1279–1288.**

Supplementary key words glycerol-3-phosphate acyltransferase • obesity • triglyceride

The first committed step in phospholipid and triacylglycerol (TG) synthesis is the formation of lysophosphatidic acid from glycerol-3-phosphate. This reaction is catalyzed by glycerol-3-phosphate acyltransferase (GPAT), and this enzyme is thought to be rate limiting for glycerophospholipid biosynthesis (1). Two unique enzymes display GPAT activity; one, microsomal GPAT, is associated with the endoplasmic reticulum (ER), and the second, the mitochondrial isoform (mtGPAT), is associated with the outer mitochondrial membrane (2). In most tissues, the mtGPAT comprises ~10% of the total activity, but in the liver, mtGPAT comprises up to 50% of the total activity (2). Activity between mtGPAT and microsomal GPAT is differentiated by their selective sensitivity to sulfhydryl group reactive reagents such as *N*-ethylmaleimide (NEM). These reagents inhibit microsomal GPAT, whereas mtGPAT activity is resistant to inhibition (3, 4). Analysis of mtGPAT-deficient mice (mtGPAT$^{-/-}$) clearly established that two separate genes encode these activities, because microsomal GPAT activity was normal in the mtGPAT$^{-/-}$ mice (5). MtGPAT has a preference for saturated fatty acyl-CoAs, especially palmitoyl-CoA, whereas microsomal GPAT does not show such substrate preferences (1, 6, 7). Because phosphatidic acid is the predominant intermediate for both phospholipid and TG synthesis, it may be that these two GPAT isoforms are involved with regulating both the amount and the fatty acid saturation of de novo synthesized phospholipids, diacylglycerols (DGs), and TGs (1).

Recent studies suggest that mtGPAT is involved in both obesity and dyslipidemia associated with obesity. MtGPAT$^{-/-}$ mice have reduced body weight and total adipose tissue weight and lower hepatic TG content, as compared with wild-type (wt) mice (5). In obese Zucker (fa/fa) rats, total GPAT activity is elevated in adipose tissue and intestine, when compared with lean rats (8), indicating that mt-

Manuscript received 13 January 2004 and in revised form 30 March 2004.

Published, JLR Papers in Press, April 21, 2004.
DOI 10.1194/jlr.M400010-JLR200

Abbreviations: CHO, Chinese hamster ovary; CPT-1, carnitine palmitoyl transferase-1; ER, endoplasmic reticulum; GPAT, glycerol-3-phosphate acyltransferase; MOI, multiplicity of infection; wt, wild type.

[1] To whom correspondence should be addressed.
e-mail: sandra.schreyer@astrazeneca.com

GPAT is induced in response to obesity. Overexpressing mtGPAT in Chinese hamster ovary (CHO) cells increases the incorporation of labeled fatty acids into TGs (9). The promotor of mtGPAT contains both sterol- and carbohydrate-responsive elements (10, 11), and mtGPAT mRNA level is upregulated by a high-carbohydrate, fat-free diet and by insulin administration to streptozotocin-diabetic mice (12). Taken together, these results show that mtGPAT activity is upregulated in tissues from obese animals or from animals fed high-carbohydrate diets and that increased activity may promote TG synthesis.

In this study, we investigated whether overexpressing mtGPAT in hepatocytes alters fatty acid metabolism and whether obesity influences hepatic mtGPAT activity. Primary rat hepatocytes were infected with control (ZsGreen) adenovirus or viruses expressing murine mtGPAT. Overexpressing mtGPAT resulted in a sharp reduction in fatty acid oxidation and a significant increase in glycerolipid synthesis. In addition, an invariant aspartic acid residue was changed to glycine [D235G] in the presumed active site within the N terminus of the enzyme (13, 14) by site-directed mutagenesis, and the activity of this enzyme was evaluated in infected cells. No activity was observed with this mutant mtGPAT, demonstrating that this residue is critical for activity. Finally, mtGPAT activity was measured in livers from lean and obese rodents and shown to be increased >2-fold in obese animals. These results support the hypothesis that increased hepatic mtGPAT activity associated with obesity contributes to increased lipid synthesis and inhibition of fatty oxidation, responses that would promote obesity itself as well as lipid disorders associated with obesity.

EXPERIMENTAL PROCEDURES

Materials

The vector pcDNA 3.1/Hygro, lipofectamine, penicillin and streptomycin, Dulbeccos' modified Eagle's medium (DMEM) with glutamax, HBSS, Williams E (WE) medium with glutamax, and fetal bovine serum (FBS) were obtained from Invitrogen (Paisley, Scotland). Fatty acid-free BSA was purchased from Research Organics (Cleveland, OH). The AdEasy adenoviral vector system, pBluescript II SK, Strataprep PCR purification kit, and QuickChange site-directed mutagenesis kit from Stratagene (La Jolla, CA) were used. ZsGreen was obtained from Clontech (Palo Alto, CA), TNT rabbit reticulocyte lysate kit from Promega (Madison, WI), DNA preparation kits from Qiagen (Hilden, Germany), isoflurane (Forene) from Abbot Scandinavia AB (Sweden), and insulin (Actrapid) from Novo Nordisk A/S (Bagsvaerd, Denmark). Collagenase type IV, lipid standards, dexamethasone, anti-FLAG M2 antibodies, and other chemicals were purchased from Sigma (St. Louis, MO). Matrigel was purchased from Collaborative Research (Bedford, MA). Restriction enzymes and Complete protease inhibitor were obtained from Roche (Mannheim, Germany). [9,10(n)-^{3}H]palmitic acid, [9,10(n)-^{3}H]oleic acid, [^{14}C]glycerol-3-phosphate, and [^{35}S]methionine were purchased from Amersham (Buckinghamshire, UK) and Ready Safe scintillant from Beckman (Fullerton, CA). The BCA protein assay kit and Super Signal West Pico Chemiluminescent substrate were purchased from Pierce (Rockford, IL). Nu-PAGE gels were obtained from Novex (San Diego, CA), immobilin P membranes from Ambion (Austin, TX), and HPLC Mix 41 from Larodan (no. 90-4010, Malmö, Sweden).

Animal experimental procedures

Female Sprague-Dawley rats, ~200 g, were obtained from Harlan Laboratories (Horst, The Netherlands). Six-week-old female C57BL/6, C57BL/6-ob/ob (referred to as ob/ob), and C57BL/6J-lean/? (referred to as lean/?) mice were obtained from Taconic M and B Laboratory (Ry, Denmark). Animals were maintained under standardized conditions of temperature (21–22°C) and humidity (40–60%), with lights on between 6 AM and 6 PM. The animals had free access to water and regular chow diet containing 12% fat, 62% carbohydrates, and 26% protein with a total energy content of 3.0 Kcal/g (R3 diet, Lactamin AB, Stockholm, Sweden). C57BL/6 mice were fed either the chow diet or a high-fat/high-sucrose (HFHS) diet (diet F1850, Bioserve, Frenchtown, NJ) for 12 weeks. The HFHS diet contained 36% fat (lard), 37% carbohydrate (mainly sucrose), and 20% protein, with a total energy content of 5.5 Kcal/g. Caloric content of the HFHS diet included 58% from fat and 27% from carbohydrate. Ob/ob and lean/? mice were analyzed at 12 weeks of age. Mice were fasted for 3 h and then anesthetized with isoflurane, and blood was collected by cardiac puncture. The livers were removed, immediately frozen in liquid nitrogen, and stored at −70°C until analysis. All animal experiments were conducted in accordance with accepted standards of humane animal care and approved by the Ethics Committee of Göteborg University.

Cloning and construction of mtGPAT-FLAG and transfection of CHO cells

A murine mtGPAT open reading frame having an FLAG epitope (DYKDDDDK) at the C terminus was cloned by polymerase chain reaction (PCR) amplification from a mouse liver cDNA library. Two PCR fragments were amplified and cloned into a pBluescript II SK vector using 5′-*Sal*I, 3′-*Not*I, and an internal *Eco*RI site (nt 1,582 from ATG). The first 1,650 bp PCR fragment was amplified using the oligonucleotides 5′-GTACCGTCGACCACCATGGAGGAGTCTTCAGTG-3′ (5′*Sal*I) and 5′-GTGACACAGTTCCCCAGAAGCTG-3′ (3′*Eco*RI). The second 978 bp fragment containing the FLAG coding sequence was amplified using the oligonucleotides 5′-GGAAGTCCTAGCTCGCGATTTCG-3′ (5′*Eco*RI) and 5′-TCGAGCGGCCGCCTACTTGTCATCATCATCCTTGTAGTCCAGCACCACAAAACTCAG-3′ (3′-*Not*I-FLAG). The sequences were confirmed by sequencing using the M13 forward/reverse primers in addition to four internal primers. The GPAT construct was subcloned into the mammalian expression vector pcDNA 3.1/Hygro using *Apa*I and *Not*I restriction enzymes. CHO cells were cultured in DMEM with 10% heat-inactivated FBS at 37°C, 5% CO_2, and 100% humidity. The cells were seeded in 10 cm culture dishes, cultured to 60–80% confluence, and transiently transfected with empty pcDNA3.1 or pcDNA3.1-mtGPAT using lipofectamine in serum-free DMEM according to the Invitrogen manual. After 4 h, 10% FBS was added, and the cells were harvested after 24 h and assayed for mtGPAT protein expression and activity.

Site-directed mutagenesis and production of recombinant adenoviruses

A D235G mtGPAT mutant construct was generated using a PCR-based site-directed mutagenesis kit (Quickchange) and the oligonucleotides 5′-GCACAGATCCCACATTG**G**CTACCTGTTGCTCACC-3′ (D235G forward) and 5′-GGTGAGCAACAGGTAG**C**CAATGTGGGATCTGTGC-3′ (D235G reverse) according to the manufacturer's instructions (mutated base in boldface type). The full-length sequence was confirmed by sequencing using the

same primers described before and recloned into pBluescript II SK. To verify that constructs remained in-frame, a coupled in vitro transcription-translation assay was performed with a TNT rabbit reticulocyte lysate system. Reactions were performed with [^{35}S]methionine and subjected to sodium dodecyl sulfate polyacrylamide gel electrophoresis followed by autoradiography. Both mitochondrial GPAT, referred to as mtGPATwt, and mutated mtGPAT, referred to as mtGPATdg, were subcloned into pShuttle-CMV using *Sal*I and *Not*I restriction enzymes and resequenced. Recombinant adenoviruses were produced by *Escherichia coli*-mediated recombination of cotransformed adenoviral backbone plasmid pAdEasy-1 and linearized pShuttle-mtGPATwt and mtGPATdg constructs. Positive clones were selected and confirmed by *Pac*I digestion. Correct clones were amplified following transformation of XL 10-Gold cells, linearized with *Pac*I, and purified using a Strataprep PCR purification kit. The packaging cell line AD-293 was grown in DMEM with 10% FBS supplemented with 100,000 IU/l penicillin and 100 mg/l streptomycin. Cells were seeded in 25 cm^2 culture flasks, cultured to 60–80% confluence, and transfected with adenoviral constructs for mtGPATwt, mtGPAT D235G, or ZsGreen using lipofectamine in DMEM without serum. After four h incubation, 10% FBS was added, and the cells were cultured for 10–14 days before harvesting. Viruses were harvested by repeated freeze/thaw cycles in 10 mM Tris, pH 8.0, centrifuged, and used for further amplification of viral stocks. Virus titer was determined using a quantitative real-time PCR (RT-PCR) method (15).

Isolation and culture of primary rat hepatocytes

Hepatocytes were prepared by a nonrecirculating collagenase perfusion (37°C and 95% O_2) through the portal vein of 200–300 g female Sprague-Dawley rats anesthetized by isoflurane inhalation. The livers were first perfused with HBSS medium supplemented with 0.6 mM EGTA, 20 mM HEPES, and 10 mM Na HCO_3. This solution was followed by WE medium supplemented with 50,000 IU/l penicillin, 50 mg/l streptomycin, 0.28 mM sodium ascorbate, 0.1 μM sodium selenite, and 400 mg/l collagenase. Cells were filtered through 250 μm and 100 μm pore size mesh nylon filters and washed three times in WE medium supplemented as described above but without collagenase and set to contain 28 mM glucose, 3 nM insulin, and 1 nM dexamethasone. The cells were cultured (200,000 cells/cm^2) in the same medium as that used for washing the cells supplemented with 10% FBS. Cells were plated for 4 h and incubated with recombinant adenoviruses for 2 h in serum-free medium. Serum-containing medium was then added without removing the viruses. Media were changed at 23 h to remove virus. For cells cultured under high-fat conditions, the media for the following 24 h also contained 150 μM oleate plus 150 μM palmitate conjugated to 0.5% BSA. In some experiments, hepatocytes were cultured on laminin-rich matrigel in serum-free medium. Similar results were obtained as compared with cells cultured on plastic, and only results from those cultured on plastic are presented here.

Mitochondrial GPAT protein expression

Total cellular proteins were isolated by homogenization in 1% Triton X-100 supplemented with Complete protease inhibitors. Mitochondrial proteins were isolated in sucrose solution containing Complete protease inhibitors as described for the GPAT assay. Protein (30 μg) was separated in 4–12% NuPage gels and transferred to immobilon P membranes, which were probed with polyclonal rabbit anti-mtGPAT antibodies directed against the murine amino acid sequence 312–326 (AgriSera, Vännäs, Sweden) or anti-FLAG M2 antibodies. The membranes were washed and incubated with horseradish peroxidase-linked donkey anti-rabbit Ig and developed using Super signal West Pico chemiluminescent substrate.

GPAT activity

Liver samples were homogenized in sucrose solution (250 mM sucrose, 10 mM Tris, pH 7.4, 1 mM EDTA, and 1 mM DTT), and nuclei were removed by centrifuging at 600 *g* for 15 min at 4°C. Supernatants were then spun at 8,000 *g* for 15 min at 4°C to pellet crude mitochondria, then at 100,000 *g* for 1 h at 4°C to pellet microsomes. Mitochondria and microsomal fractions were then tested for GPAT activity in the presence and absence of 2 mM NEM. Subsequent analysis of these fractions demonstrated that the mitochondrial fraction still contained significant amounts of ER protein. Thus, the NEM-resistant activity for mitochondrial and microsomal pellets was pooled and assigned as mitochondria activity (Table 2). Similarly, the NEM-sensitive activity for both pellets was pooled and assigned as microsomal activity. For assays with cultured hepatocytes, cells were rinsed in PBS, lysed in sucrose solution, and centrifuged to pellet nuclei; then the supernatant was centrifuged at 100,000 *g* to obtain both microsomes and mitochondria. Pellets were then tested for NEM-sensitive and NEM-resistant GPAT activity. The use of NEM sensitivity on a single high-speed spin pellet has been previously demonstrated to effectively differentiate mitochondrial from ER-associated GPAT activity (4, 9, 16–18).

GPAT activity on pelleted protein fractions was performed similarly to that described by Yet et al. (19). The assay buffer contained 75 mM Tris, pH 7.5, 4 mM $MgCl_2$, 8 mM NaF, 100 μM palmitoyl-CoA, 500 μM [^{14}C]glycerol-3-phosphate (0.5 μCi/reaction), and 2 mg/ml BSA. The reaction was started by mixing 15 μg of protein with the assay buffer in a final volume of 200 μl and shaking the samples for 20 min at room temperature. To measure NEM-resistant GPAT activity ("mitochondrial GPAT activity"), protein samples were mixed with NEM (2 mM final concentration) for 15 min at 4°C before starting the reaction. Microsomal GPAT activity ("ER GPAT activity") was determined by subtracting mitochondrial activity from total activity. Reactions were stopped by adding 1 ml of water-saturated butanol, which extracts the GPAT product but not the radioactive substrate. Samples were vortexed, and the butanol phase was rinsed twice with butanol-saturated water prior to adding scintillant and counting for radioactivity.

β-oxidation

Cells were incubated in control medium or infected with virus as described earlier. The medium was then changed to serum-free WE medium containing 3 nM insulin, 1 nM dexamethasone, and either 300 μM palmitic acid plus 1 μCi [9,10(n)-^{3}H]palmitic acid/ml or 300 μM oleic acid containing 1 μCi [9,10(n)-^{3}H]oleic acid/ml oleic acid. Fatty acids were complexed to 0.5% fatty acid-free BSA. After the given incubation period at 37°C, the medium was removed and mixed with concentrated perchloric acid (0.5% final volume) plus BSA (2% final volume) to precipitate the labeled fatty acids. Samples were vortexed and centrifuged (5,000 rpm for 5 min), and a second round of BSA-mediated fatty acid precipitation was performed. Radioactivity was determined in the supernatant to measure water-soluble β-oxidation products.

Lipid biosynthesis

Hepatocytes were incubated with radioactive palmitate or oleate as described above. Cells were rinsed with PBS and scraped from the plates using PBS containing 1% Triton X-100. Lipids were extracted from either the cellular homogenate or the media in methanol-chloroform (1:2) (20) followed by a second chloroform extraction, and samples were subjected to thin-layer chromatography for separation. To separate neutral lipids, hexane-diethyl ether-acetic acid (80:20:1) or petroleum ether-diethyl ether-acetic acid (70:30:1) was used, whereas chloroform-metha-

nol-acetic acid-water (25:15:4:2) was used to separate polar lipids. Lipids were visualized with iodine vapor and compared with known standards. The radioactivity incorporated into lipids was determined by scraping corresponding bands into scintillation vials and counting radioactivity.

RNA quantification

Mouse GPAT was quantified from liver samples using RT-PCR. RNA was isolated from liver samples using Trizol (Invitrogen, Carlsbad, CA) following the manufacturer's instructions. cDNA was then synthesized using the Invitrogen Superscript synthesis system. Samples were quantified for mouse GPAT mRNA with the following primers, obtained from Applied Biosystems UK (Cheshire, UK): GPAT forward, 5′-GGCTTGAGAGCTGCCACCT-3′; probe, VIC 5′-TAGTGCGGCCAGTGACTGCTTCAAGA-3′ TAMRA; GPAT reverse, 5′-AGCCCTTTAGCTGTTGGGAAG-3′.

Samples were quantified using an Applied Biosystems 7700 sequence detector (Foster City, CA) and corrected to the expression of the endogenous control, acidic ribosomal phosphoprotein P0 (36B4) using the following primers: 36B4 forward, 5′-GAGGAATCAGATGAGGATATGGGA-3′; probe, VIC 5′-TCGGTCTCTTCGACTAATCCCGCCAA-3′ TAMRA; and 36B4 reverse, 5′-AAGCAGGCTGACTTGGTTGC-3′.

Total lipid mass measurements

Following extraction of lipids (20), samples were dissolved with a mix of solutions A and B (see below) at a ratio of 9:1. The mobile phase was created by a combination of three solvent mixtures: A) heptane-tetrahydrofuran (99:1, v/v); B) acetone-dichloromethane (2:1; v/v); and C) isopropanol-water (85:15, v/v) containing 7.5 mM acetic acid and 7.5 mM ethanolamine. Samples were separated on an HPLC system using a Waters spherisorb, 5 μm silica column (4.6 × 100 mm, no. 830112, Sorbent AB, Sweden). Lipids were detected with a PL-ELS 1000 Evaporative Light Scattering Detector from Polymer Laboratories, and HPLC Mix 41 was used as the standard.

Statistics

Values are expressed as mean ± SEM. All experiments were repeated two to four times using different rat hepatocyte perfusions, and representative experiments are presented. Comparisons between means were made by ANOVA. ANOVA was followed, when appropriate, by Tukey's posthoc test to do pair-wise comparisons between all groups. Student's *t*-test was used to evaluate pairwise comparisons.

RESULTS

Cloning of mtGPAT and overexpression in CHO cells

To study the effect of overexpressing mtGPAT, murine mtGPAT was cloned and linked with a FLAG epitope at the C terminus. To verify that our construct was properly expressing mtGPAT, CHO cells were transiently transfected with mtGPAT in a pcDNA expression vector (pmtGPAT) and compared with cells transfected with an empty vector (pEmpty). Total cellular proteins and mitochondrial proteins were prepared, and the mtGPAT protein level was assayed with Western blot using antibodies directed against either the FLAG epitope (**Fig. 1A**) or antibodies generated against aa 312-326 in mouse mtGPAT (Fig. 1B). The mtGPAT protein was not detectable in pEmpty-transfected cells but was highly induced by overexpressing the enzyme, and the expression level was enriched using a mitochondrial protein preparation (Fig. 1A, B). Increased mtGPAT expression was detected using both antibodies, but the anti-mtGPAT antibody gave a cleaner result with less nonspecific binding. Total GPAT activity increased >4-fold in response to mtGPAT overexpression ($P < 0.05$), and the increase was due to increased mtGPAT activity, measured as NEM-resistant GPAT activity ($P < 0.01$) (Fig. 1C). These results are consistent with results obtained in other studies overexpressing mtGPAT in CHO cells (9, 19) and thus confirm that our construct is in frame and that our anti-mtGPAT antibodies readily detect mtGPAT.

Overexpression of mtGPAT and a mutant mtGPAT in primary rat hepatocytes

Recombinant adenoviruses expressing either the control construct, ZsGreen (AdZsGreen), or mtGPAT (AdmtGPATwt), under the CMV promoter, were produced. Primary rat hepatocytes were isolated and infected with the respective viruses. Minimal fluorescence in AdZsGreen-infected cells was observed for the first 18 h, after which expression increased through 48 h of culture (**Fig. 2A**). Thus, all of the following experiments were conducted 48 h after infection of the cells.

Mitochondrial proteins were isolated, and the mtGPAT protein level was measured in the cells infected with the different constructs. As shown in Fig. 2B, mtGPAT protein level was comparable in uninfected and AdZsGreen-infected cells. However, infection with AdmtGPATwt resulted in a dramatic increase in mtGPAT protein expression. Overexpressing mtGPAT increased total GPAT activity 2-fold, as compared with uninfected cells or AdZsGreen-infected cells ($P < 0.05$) (Fig. 2C). The increased activity was due entirely to a 2.7-fold increased mtGPAT activity ($P < 0.0001$ vs. AdZsGreen-infected or noninfected cells).

Along with overexpressing wt mtGPAT protein, we aimed to identify amino acid domains of mtGPAT critical for activity. Studies in bacteria have demonstrated that aspartic acid D311 is critical for activity (13, 14). Because the homology in this region is conserved between several species, a corresponding mutation was introduced in the murine mtGPAT construct, changing aspartic acid 235 to a glycine residue (D235G). The mtGPAT protein level was then compared in cells infected with 20 multiplicity of infection (MOI) of either AdmtGPATwt or the mutant protein, AdmtGPATdg. Results show that AdmtGPATdg protein was expressed, although expression levels were slightly lower than those observed in AdmtGPATwt-infected cells (Fig. 2B). When cells were infected with a five-times-higher titer (100 MOI; AdmtGPATdg-ht), a much higher protein expression than 20 MOI of either AdmtGPATwt or AdmtGPATdg was observed (Fig. 2B). Despite showing high protein expression, AdmtGPATdg had no effect on GPAT activity, even when administered at the high titer (Fig. 2C). Thus, this single amino acid substitution gives rise to an inactive enzyme.

Effect of overexpressing mtGPAT on β-oxidation

To study the effect of overexpression of mtGPAT on fatty acid oxidation, infected hepatocytes were incubated

for 1 h with [^{3}H]palmitic acid, and the water-soluble β-oxidation products were assayed in the media (**Fig. 3A**). Hepatocytes infected with AdmtGPATwt had an 81% reduction in palmitate oxidation, as compared with AdZsGreen-infected cells ($P < 0.05$). After a 2 h pulse, we observed a similar reduction in palmitate oxidation (AdZsGreen: 14.6 ± 1.0 nmol/mg; AdmtGPATwt: 2.9 ± 0.8 nmol/mg; $P < 0.001$), and dramatic differences continued through 4 h. Hepatocytes infected with AdmtGPATdg showed no difference in oxidation, as compared with AdZsGreen-infected cells, again demonstrating that this mutation results in an inactive enzyme (Fig. 3A). Finally, infected hepatocytes were lipid loaded by incubating them for 24 h with 300 μM oleic acid-palmitic acid (1:1) and then tested for fatty acid oxidation using either [^{3}H]oleic acid or [^{3}H]palmitic acid. As shown in Fig. 3B, lipid-loaded hepatocytes infected with AdmtGPATwt had decreased oleate oxidation, as compared with AdZsGreen-infected cells and the difference was maintained during all time-points examined. Similar results were observed for cells pulsed with [^{3}H]palmitic acid (7.8 ± 0.3 nmol/mg/hr for AdZsGreen vs. 1.3 ± 0.2 nmol/mg/hr for AdmtGPATwt; $P < 0.0001$). Results demonstrate that under both low and high fatty acid concentrations and regardless of the radiolabeled fatty acid tracer utilized, overexpression of mtGPAT impairs fatty acid oxidation.

Effects of overexpressing mtGPAT on lipid biosynthesis

Because fatty acid oxidation was impaired in mtGPAT-overexpressing hepatocytes, we investigated whether this also resulted in increased de novo lipid biosynthesis. Hepatocytes were incubated with [^{3}H]palmitic acid, and radioactive cellular DG, TG, and phosphatidylcholine (PC) were measured (**Fig. 4A**). Cells infected with AdmtGPATwt showed a significant increase in intracellular DG synthesis ($P < 0.001$). In a separate study, the difference in DG synthesis was even greater after a 2 h pulse period, where AdZsGreen-infected cells showed 5.9 ± 0.5 nmol/mg whereas AdmtGPAT-infected cells showed 27.2 ± 7.5 nmol/mg DG synthesized ($P < 0.01$). Thus, the overexpression of mtGPAT greatly enhances the de novo synthesis of DG. A 28% increase in PC synthesis in mtGPAT-over-

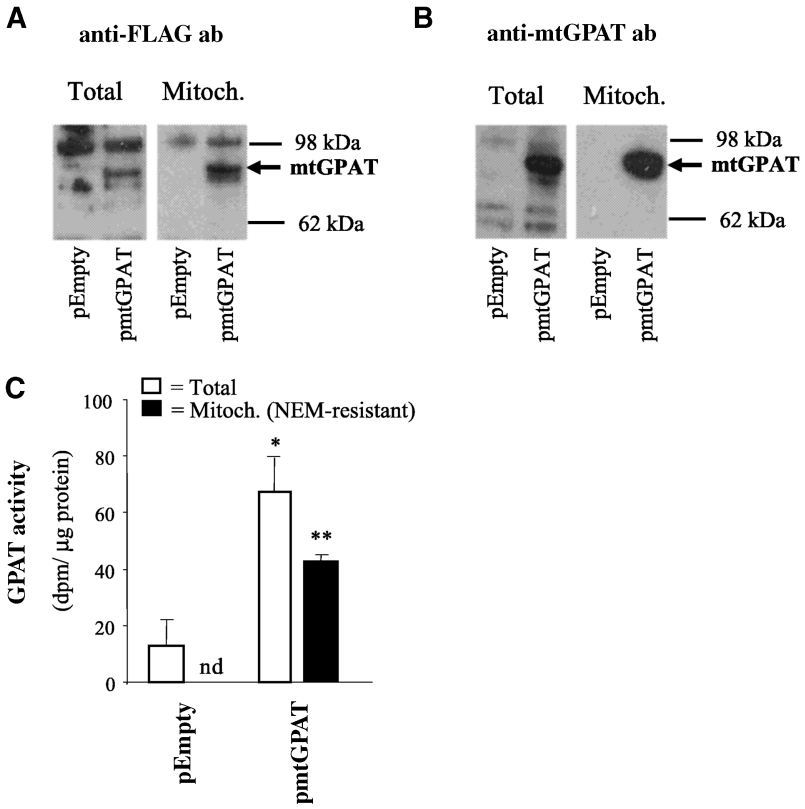

Fig. 1. The effect of overexpression of the mitochondrial isoform of glycerol-3-phosphate acyltransferase (mtGPAT) in Chinese hamster ovary (CHO) cells on mtGPAT expression and activity. CHO cells were transiently transfected with either an empty pcDNA 3.1 vector (pEmpty) or a vector containing full-length mtGPAT with a FLAG sequence at the C terminus (pmtGPAT). After 24 h, the cells were harvested and assayed for mtGPAT protein and GPAT activity. A: Western immunoblot results using antibodies directed against the FLAG epitope. B: Western immunoblot results using antibodies generated against mouse mtGPAT aa 312-326. C: Total and mtGPAT activity in cellular homogenates. Total membrane fractions were assayed for total GPAT activity in the absence and for mtGPAT activity in the presence of 2 mM *N*-ethylmaleimide (NEM) as described in Experimental Procedures. A representative result from three independent experiments is presented. Values are presented as the mean ± SEM (n = 3). *$P < 0.05$, **$P < 0.01$ versus pEmpty-transfected cells (Student's *t*-test).

expressing cells, as compared with AdZsGreen-infected cells, was also observed ($P < 0.05$, Fig. 4A). In contrast, the amount of labeled TG was not influenced by mtGPAT overexpression (Fig. 4A), with synthesis rates of ~20 nmol/mg/hr. These results suggest that the radiolabeled DG is being directed more toward phospholipid synthesis than TG synthesis. The intracellular cholesteryl ester radioactivity was low and did not differ between AdmtGPATwt- and AdZsGreen-infected cells (data not shown).

We next investigated whether overexpression of mtGPAT would affect glycerolipid biosynthesis in lipid-loaded hepatocytes. Infected hepatocytes were incubated for 24 h with 300 μM oleic acid/palmitic acid (see Experimental Procedures) and then with [^{3}H]oleic acid over the subsequent 6 h tracing period (Fig. 4B). Similar to our findings with cells cultured in normal media, increased DG and PC synthesis was observed when mtGPAT was overexpressed. Similar results were observed when [^{3}H]palmitate was utilized as the tracer (data not shown). However, in contrast to cells cultured in normal media, we observed increased TG synthesis in lipid-loaded hepatocytes infected with AdmtGPATwt virus, as compared with the control virus (Fig. 4B). Thus, under conditions that favor TG synthesis, such as elevated fatty acid concentrations in the media, overexpression of mtGPAT results in increased de novo TG synthesis. Under normal culture conditions, the amount of labeled TG secreted to the culture medium was very low, so possible differences in TG secretion in response to mtGPAT overexpression could not be ascertained. However, in cells cultured with high fatty acids, we observed a modest increase in TG secretion after 4 h in response to mtGPAT overexpression (AdZsGreen: 0.48 ± 0.13 nmol/mg; AdmtGPATwt: 1.28 ± 0.35 nmol/mg; $P = 0.06$).

To ascertain whether AdmtGPATwt-infected hepatocytes have increased lipid accumulation, intracellular total lipid mass was measured in cells cultured for 24 h with or without 300 μM oleic acid/palmitic acid (**Table 1**). Lipid loading of the cells resulted in a 1.7–2.3-fold increase in intracellular DG and TG. Under normal culture media (non-lipid loading), AdmtGPATwt-infected hepatocytes had elevated levels of DG but not TG, as compared with AdZsGreen-infected cells (Table 1). Following lipid loading of the cells, both intracellular DG and TG levels were significantly increased in response to mtGPAT overexpression (Table 1). The intracellular phospholipid and cholesteryl ester total mass was not influenced by mtGPAT overexpression (data not shown). Thus, results were in good overall agreement with the results obtained for measuring de novo synthesis of these lipids.

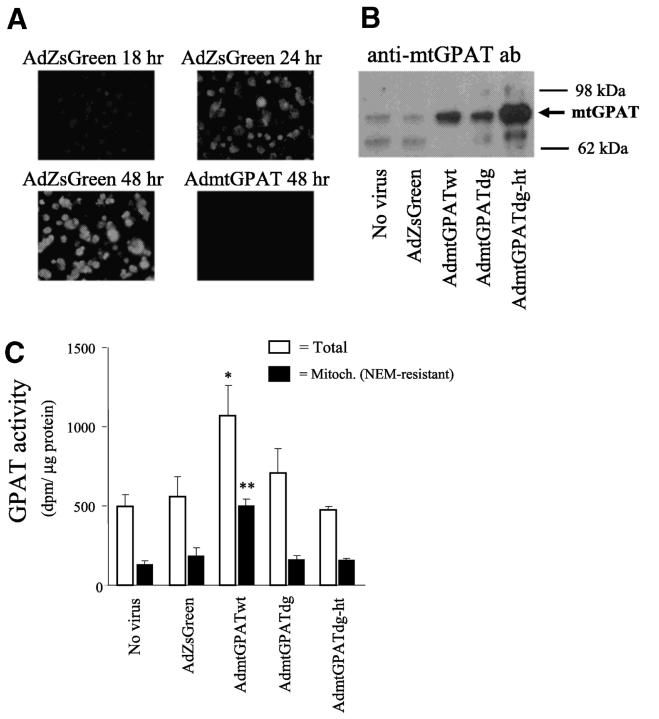

Fig. 2. Wild-type (wt) and D235G mtGPAT expression and activity in primary rat hepatocytes. Primary cultures of rat hepatocytes were cultured with either no virus or with 20 multiplicity of infection (MOI) of AdZsGreen, AdmtGPATwt, or AdmtGPATdg. A higher adenoviral titer of AdmtGPATdg was also used (titer = 100 MOI, AdmtGPATdg-ht). A: The green fluorescence of AdZsGreen-infected hepatocytes was followed up to 48 h postinfection. AdmtGPAT-infected cells were used as controls for fluorescence. B: MtGPAT protein level was analyzed with Western blot using anti-mtGPAT antibodies. C: Total and mtGPAT activity in cellular homogenates. Membrane fractions were assayed for total and mtGPAT activity by performing the reaction in the absence or presence of 2 mM NEM, respectively. A representative result from four independent liver perfusions is presented. Values are presented as the mean ± SEM (n = 3). *$P < 0.05$, **$P < 0.0001$ versus all other groups (one-way ANOVA followed by Tukey's test).

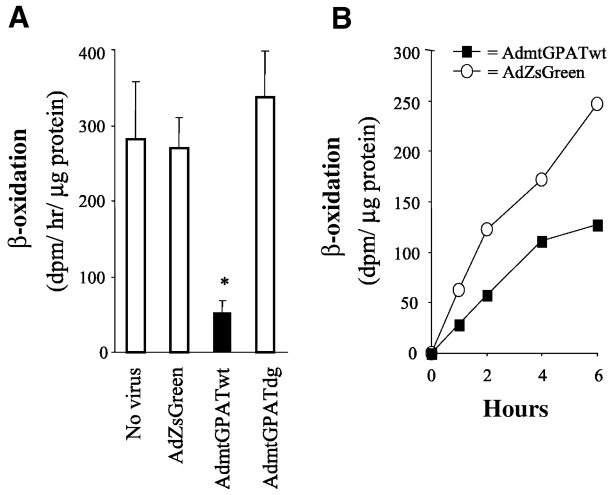

Fig. 3. Fatty acid oxidation in response to mtGPAT overexpression in primary rat hepatocytes. Rat hepatocytes were cultured with either no virus or with 20 MOI of AdZsGreen, AdmtGPATwt, or AdmtGPATdg. A: Cells were labeled with [9,10(n)-^{3}H]palmitic acid for 1 hr before analyzing for oxidation. B: Cells were preloaded with 300 μM oleic acid-palmitic acid (1:1) for 24 h and then labeled for 1, 2, 4, or 6 h with [9,10(n)-^{3}H]oleic acid. Fatty acid oxidation was analyzed as described in Experimental Procedures. For panel A, a representative result from three independent liver perfusions is presented and values are presented as the mean ± SEM (n = 3). For panel B, values are presented as the mean (n = 2). *$P < 0.05$ versus all other groups (one-way ANOVA followed by Tukey's test).

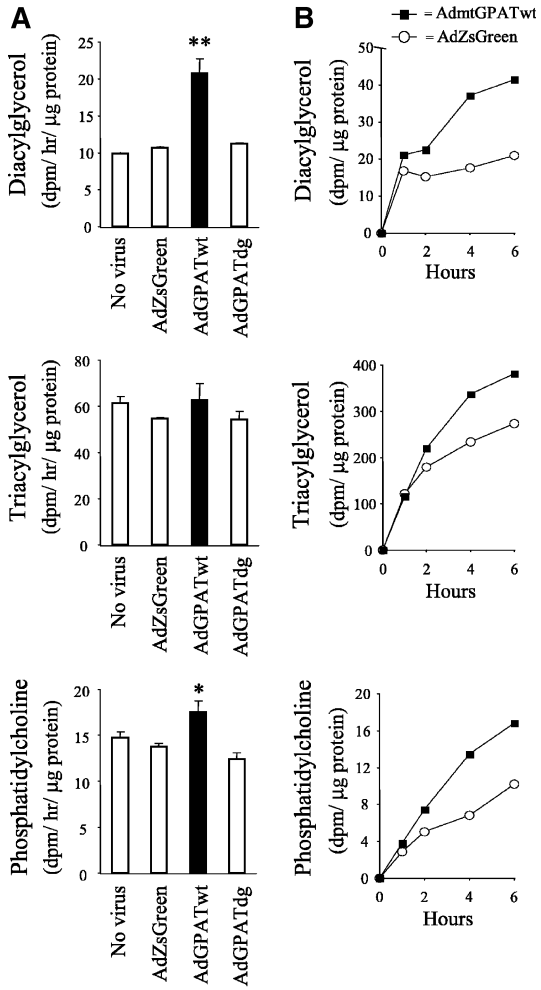

Fig. 4. The effect of overexpression of mtGPAT in primary rat hepatocytes on lipid biosynthesis. Primary cultures of rat hepatocytes were cultured with either no virus or with 20 MOI of AdZsGreen, AdmtGPATwt, or AdmtGPATdg. A: Cells were labeled with [9,10(n)-^{3}H]palmitic acid for 1 hr before analyzing for cellular lipid radioactivity. B: Cells were preloaded with 300 µM oleic acid-palmitic acid (1:1) for 24 h and then labeled for 1, 2, 4, or 6 h with [9,10(n)-^{3}H]oleic acid. Cellular lipids were extracted and isolated by thin-layer chromatography as described in Experimental Procedures. For panel A, a representative result from three independent liver perfusions is presented and values are presented as the mean ± SEM (n = 3). For panel B, values are presented as the mean (n = 2). *$P < 0.05$ versus AdZsGreen- and AdmtGPATdg-infected cells and **$P < 0.001$ versus all other groups (one-way ANOVA followed by Tukey's test).

TABLE 1. Intracellular diacylglycerol (DG) and triacylglycerol (TG) concentrations in primary rat hepatocytes in response to lipid loading and to infection with control virus or mtGPAT virus

	Non-Lipid Loaded		Lipid Loaded	
	DG	TG	DG	TG
	µg/mg Protein			
AdZsGreen	0.43 ± 0.06	120 ± 1	1.00 ± 0.08[a]	205 ± 13[a]
AdmtGPATwt	0.88 ± 0.03	131 ± 4	2.29 ± 0.12[a]	256 ± 9[a]
P	<0.01	NS	<0.001	<0.01

Primary cultures of rat hepatocytes were cultured with either AdZsGreen or AdmtGPAT wild type (AdmtGPATwt) for 19 h. During the following 24 h, the cells were cultured in either standard medium supplemented with glucose and 10% fetal bovine serum (non-lipid loaded) or the same media containing 300 µM oleic acid-palmitic acid (1:1) conjugated to 0.5% BSA (lipid loaded). Intracellular lipids were extracted and analyzed using an HPLC system as described in Experimental Procedures. Values are presented as the mean ± SEM (n = 3).

[a] $P < 0.05$ versus non-lipid-loaded cells. NS, not significant.

Effect of obesity on mtGPAT activity in the liver

Because overexpressing mtGPAT reduced β-oxidation and increased glycerolipid biosynthesis, we hypothesized that there may be dysregulation of mtGPAT activity in livers from obese rodents and that this may contribute to the hepatic lipid accumulation seen in such animals. The influence of diet-induced obesity and genetic obesity on hepatic GPAT expression and activity was investigated. C57BL/6 mice were fed regular chow or an HFHS diet for 12 weeks, and hepatic GPAT expression and activity were analyzed. In addition, GPAT expression and activity were analyzed in 12-week-old lean/? or ob/ob mice, the latter of which are deficient in leptin and display gross obesity, even when maintained on low-fat diets. As expected, the body weights were elevated in both HFHS diet obese and ob/ob mice, compared with corresponding lean controls (**Table 2**). Plasma triglycerides were increased in ob/ob mice but decreased in HFHS diet obese mice. In addition, both plasma insulin and glucose levels were elevated in both models of obesity (data not shown). Total GPAT activity tended to increase (55%) in HFHS diet obese mice and was markedly elevated in ob/ob mice (2.5-fold, $P < 0.05$), as compared with corresponding lean controls (Table 2). For the diet-induced obese mice, there was a 2.2-fold increase in mtGPAT activity ($P < 0.001$) and a trend toward increased ER GPAT activity, as compared with lean controls. In ob/ob mice, there was an increase in both mtGPAT activity (2.3-fold, $P < 0.05$) and ER GPAT activity (2.5-fold, $P < 0.001$), as compared with their lean counterparts. Thus, in two different obesity models, mtGPAT activity was upregulated in the liver; but only under severe obesity, as seen in the ob/ob mouse, was ER GPAT activity significantly upregulated. To confirm that obesity increases mtGPAT activity, we measured mtGPAT mRNA and protein levels using RT-PCR and Western blot methods, respectively. As compared with C57BL/6 mice, ob/ob mice showed a 5.5-fold increase in mtGPAT mRNA levels ($P = 0.002$, data not shown). Short-term feeding (2 weeks) of the HFHS diet also increased hepatic mtGPAT mRNA levels 1.6-fold, although differences were not statistically significant. Western blot analysis of liver samples from chow diet- versus HFHS-fed mice and lean/? versus ob/ob mice demonstrated that mtGPAT protein is elevated in genetically obese but not diet-induced obese mice, as compared with their lean counterparts (**Fig. 5**). Thus, in ob/ob mice, increased mtGPAT activity reflects increases in both mRNA and protein levels, whereas in diet-induced obese mice, the increased activity results from posttranslational regulation. The latter results are in agreement with a published report demonstrating discordance between mtGPAT expression, protein levels, and activity in response to dietary treatment (21).

TABLE 2. Body weights, plasma triglyceride levels, and hepatic GPAT activity from lean and obese mice

Animals	Body Weight	Plasma Triglycerides	GPAT Activity		
			Total	Endoplasmic Reticulum	Mitochondrial
	g	*mM*	*% lean total activity*		
Lean (n = 5)	23.7 ± 2.2	0.5 ± 0.1	100 ± 20	71 ± 21	29 ± 3
Diet obese (n = 5)	40.7 ± 3.3[a]	0.3 ± 0.1[b]	155 ± 31	92 ± 32	63 ± 7[a]
Lean/? (n = 8)	20.7 ± 1.1	0.8 ± 0.3	100 ± 20	79 ± 21	21 ± 3
ob/ob (n = 7)	50.2 ± 2.0[a]	2.6 ± 1.7[b]	245 ± 16[a]	197 ± 17[a]	48 ± 9[b]

Female C57BL/6 mice were fed regular chow (lean) or a high-fat/high-sucrose diet (diet obese) for 12 weeks and then fasted for 3 h prior to the collection of plasma and livers. Twelve-week-old lean (lean/?) or ob/ob female mice were also evaluated. Liver total, endoplasmic reticulum (ER) (*N*-ethylmaleimide [NEM]-sensitive), and mitochondrial (NEM-resistant) glycerol-3-phosphate acyl transferase (GPAT) activities were measured as described in Experimental Procedures. The GPAT activities (total, ER, and mitochondrial) are given as percentage of corresponding lean total GPAT activity. The values are presented as the mean ± SEM.

[a] $P < 0.001$ versus lean mice (Student's *t*-test).

[b] $P < 0.05$ versus lean mice (Student's *t*-test).

DISCUSSION

In most tissues, mtGPAT contributes minimally to total GPAT activity, whereas in the liver, it constitutes up to 50% of total activity (2, 21). Thus, mtGPAT may have a unique role in handling hepatic fatty acids in response to nutrient status. By overexpressing mtGPAT in primary cultures of rat hepatocytes, we were able to study how mtGPAT affects the partitioning of fatty acids into different lipid moieties and whether this enzyme influences fatty acid oxidation. We showed that in response to mtGPAT overexpression, fatty acids are directed away from oxidation and into glycerolipid synthesis. Thus, mtGPAT can be considered a driving force for increased hepatic lipid synthesis and accumulation in obesity.

In states of nutrient excess in which there are high circulating insulin and low glucagon levels, hepatic de novo lipogenesis is upregulated while fatty acid oxidation is reduced (22–24). Activation of lipogenic pathways and suppression of fatty acid oxidation are also observed in obesity (25, 26). Insulin treatment or carbohydrate-rich diets upregulate hepatic mtGPAT activity in vivo (12). In this study, we show that obesity also increases hepatic mtGPAT activity. Similar to mtGPAT, acetyl-CoA carboxylase is upregulated in response to carbohydrate-rich diets (27) and in the obese state (28). Increased acetyl-CoA carboxylase activity increases malonyl-CoA concentrations; this increase, in turn, inhibits carnitine palmitoyl transferase-1 (CPT-1), leading to reduced fatty acid oxidation (29, 30). Both CPT-1 and mtGPAT are located on the mitochondrial outer membrane (31–33), suggesting that they compete for the same pool of fatty acids for utilization in mitochondrial oxidation or glycerolipid synthesis, respectively. Our results demonstrate that overexpression of mtGPAT decreases fatty acid oxidation, supporting the concept that mtGPAT can compete fatty acids away from CPT-1. Therefore, decreased hepatic β-oxidation associated with obesity may result from a combination of reduced CPT-1 activity and selective partitioning of fatty acids away from CPT-1 and into glycerolipid synthesis via mtGPAT. Whether this occurs in tissues other than liver remains to be determined.

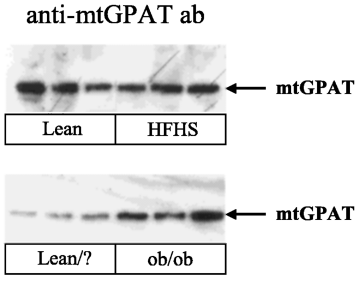

Fig. 5. Hepatic mtGPAT protein expression in lean and obese mice. Female C57BL/6 mice were fed regular chow (Lean) or a high-fat/high-sucrose (HFHS) diet for 12 weeks. Twelve-week-old lean (Lean/?) or ob/ob female mice were also evaluated. Western immunoblot was performed on equivalent amounts of liver homogenate using antibodies generated against mouse mtGPAT aa312-326 as described in Experimental Procedures.

In this study, overexpression of mtGPAT increased DG, TG, and phospholipid biosynthesis. However, the increase in TG synthesis was seen only in cells provided with additional fatty acids. This suggests that triglyceride synthesis is not necessarily the default endpoint when glycerolipid synthesis is promoted. Indeed, our results suggest that PC synthesis is the primary default pathway induced in response to mtGPAT overexpression. In HEK 293 cells transiently transfected with mtGPAT, increased incorporation of labeled oleate into both TG and phospholipids is observed (9). However, when transfections were done in CHO cells, TG biosynthesis increased, whereas the PC biosynthesis was decreased (9). Differences may reflect the altered capabilities of nonhepatic cell lines to respond to increased lipid synthesis. Studying the overexpression of mtGPAT in hepatocytes, a cell whose major function is to regulate the synthesis and secretion of these lipids, more clearly defines the actual role of mtGPAT in lipid partitioning.

Surprisingly, increased glycerolipid biosynthesis was seen in response to mtGPAT overexpression when using either palmitic acid or oleic acid as radioactive tracers, indicating that mtGPAT can utilize both saturated and monounsaturated fatty acids. Numerous studies have demonstrated that mtGPAT prefers palmitic acid over other

saturated or unsaturated fatty acids (1, 6, 7). Our findings suggest that this preference may not be reflected in the intact cell. Indeed, it has recently been shown that mtGPAT substrate preference depends partially on fatty acid binding protein availability (34). In that study, mtGPAT substrate preference depended on the availability of albumin or acyl-CoA binding protein in the assay media. Thus, the cellular fatty acid/fatty acid binding protein concentrations may influence mtGPAT activity more than does fatty acid composition.

There is growing evidence that GPAT activity is upregulated in multiple tissues from obese animals. In obese Zucker (fa/fa) rats, total GPAT activity is elevated in adipose tissue and intestine (8) and in pancreatic β-cells (35), as compared with lean rats. We show that mtGPAT activity is upregulated in livers from two different mouse models of obesity. In the HFHS diet-induced obese mice, mtGPAT activity was increased but protein levels were unchanged. A discordance between mtGPAT activity and protein expression in rat tissues in response to dietary treatment has been reported (21), suggesting that mtGPAT activity may be regulated posttranslationally. However, in livers of severely obese (ob/ob) mice, mtGPAT mRNA, protein, and activity were all increased. Possible explanations for this are that a threshold of obesity is required before mtGPAT mRNA levels are increased or that leptin deficiency upregulates the expression of this gene.

The extent of increased mtGPAT activity we observed in mtGPAT-overexpressing hepatocytes was comparable with the in vivo induction in response to obesity. This suggests that results obtained from the in vitro studies are metabolically consistent with what may be occurring in vivo. Thus, increased mtGPAT activity associated with obesity likely contributes to increased fat synthesis and deposition, a process that would further contribute to obesity.

Alignment of various membrane-bound glycerolipid acyltransferases from different species and mutagenesis studies of bacterial GPAT (13, 14) and murine mtGPAT (36) have demonstrated that a highly conserved region in the N terminus (aa 224-318) is critically important for GPAT activity. Using site-directed mutagenesis of bacterial GPAT, an invariant aspartic acid residue in the N terminus was shown to be of importance for GPAT activity (13, 14). In this study, the corresponding and conserved murine aspartic acid D235 was found to be critical for mtGPAT function in rat hepatocytes. Thus, in addition to a highly conserved arginine residue, R318 (36), D235 is required for murine mtGPAT activity. These findings help define domains of mtGPAT that may be targets for inhibition to reduce cellular mtGPAT activity.

The results presented here help identify mtGPAT as a major regulator of fatty acid partitioning in hepatocytes and suggest that this enzyme may be involved in promoting lipid synthesis. The upregulation of mtGPAT in livers from obese rodents is consistent with the involvement of mtGPAT in fatty liver and may contribute to hyperlipidemia in states of nutrient excess. Elevated hepatic mtGPAT associated with obesity may contribute to increased lipid synthesis and inhibition of fatty oxidation, responses that would drive obesity itself and lipid disorders associated with obesity. These findings suggest that inhibiting mtGPAT may be beneficial in reducing hepatic lipid accumulation by promoting hepatic β-oxidation.

REFERENCES

1. Dircks, L. K., and H. S. Sul. 1997. Mammalian mitochondrial glycerol-3-phosphate acyltransferase. *Biochim. Biophys. Acta.* **1348:** 17–26.
2. Bell, R. M., and R. A. Coleman. 1980. Enzymes of glycerolipid synthesis in eukaryotes. *Annu. Rev. Biochem.* **49:** 459–487.
3. Bates, E. J., D. L. Topping, S. P. Sooranna, D. Saggerson, and P. A. Mayes. 1977. Acute effects of insulin on glycerol phosphate acyl transferase activity, ketogenesis and serum free fatty acid concentration in perfused rat liver. *FEBS Lett.* **84:** 225–228.
4. Saggerson, E. D., C. A. Carpenter, C. H. K. Cheng, and S. R. Sooranna. 1980. Subcellular distribution and some properties of N-ethylmaleimide-sensitive and -insensitive forms of glycerol phosphate acyltransferase in rat adipocytes. *Biochem. J.* **190:** 183–189.
5. Hammond, L. E., P. A. Gallagher, S. Wang, S. Hiller, K. D. Kluckman, E. L. Posey-Marcos, N. Maeda, and R. A. Coleman. 2002. Mitochondrial glycerol-3-phosphate acyltransferase-deficient mice have reduced weight and liver triacylglycerol content and altered glycerolipid fatty acid composition. *Mol. Cell. Biol.* **22:** 8204–8214.
6. Bates, E. J., and E. D. Saggerson. 1979. A study of the glycerol phosphate acyltransferase and dihydroxyacetone phosphate acyltransferase activities in rat liver mitochondrial and microsomal fractions. Relative distribution in parenchymal and non-parenchymal cells, effects of N-ethylmaleimide, palmitoyl-coenzyme A concentration, starvation, adrenalectomy and anti-insulin serum treatment. *Biochem. J.* **182:** 751–762.
7. Monroy, G., F. H. Rola, and M. E. Pullman. 1972. A substrate- and position-specific acylation of sn-glycerol 3-phosphate by rat liver mitochondria. *J. Biol. Chem.* **247:** 6884–6894.
8. Jamdar, S. C., and W. F. Cao. 1995. Triacylglycerol biosynthetic enzymes in lean and obese Zucker rats. *Biochim. Biophys. Acta.* **1255:** 237–243.
9. Igal, R. A., S. Wang, M. Gonzalez-Baro, and R. A. Coleman. 2001. Mitochondrial glycerol phosphate acyltransferase directs the incorporation of exogenous fatty acids into triacylglycerol. *J. Biol. Chem.* **276:** 42205–42212.
10. Ericsson, J., S. M. Jackson, J. B. Kim, B. M. Spiegelman, and P. A. Edwards. 1997. Identification of glycerol-3-phosphate acyltransferase as an adipocyte determination and differentiation factor 1- and sterol regulatory element-binding protein-responsive gene. *J. Biol. Chem.* **272:** 7298–7305.
11. Jerkins, A. A., W. R. Liu, S. Lee, and H. S. Sul. 1995. Characterization of the murine mitochondrial glycerol-3-phosphate acyltransferase promoter. *J. Biol. Chem.* **270:** 1416–1421.
12. Shin, D. H., J. D. Paulauskis, N. Moustaid, and H. S. Sul. 1991. Transcriptional regulation of p90 with sequence homology to Escherichia coli glycerol-3-phosphate acyltransferase. *J. Biol. Chem.* **266:** 23834–23839.
13. Lewin, T. M., P. Wang, and R. A. Coleman. 1999. Analysis of amino acid motifs diagnostic for the sn-glycerol-3-phosphate acyltransferase reaction. *Biochemistry.* **38:** 5764–5771.
14. Heath, R. J., and C. O. Rock. 1998. A conserved histidine is essential for glycerolipid acyltransferase catalysis. *J. Bacteriol.* **180:** 1425–1430.
15. Ma, L., H. A. Bluyssen, M. de Raeymaeker, V. Laurysens, N. van der Beek, H. Pavliska, A. J. van Zonneveld, P. Tomme, and H. H. van Es. 2001. Rapid determination of adenoviral vector titers by quantitative real-time PCR. *J. Virol. Methods.* **93:** 181–188.
16. Nimmo, H. G., and B. Houston. 1978. Rat adipose-tissue glycerol phosphate acyltransferase can be inactivated by cyclic AMP-dependent protein kinase. *Biochem. J.* **176:** 607–610.
17. Muoio, D. M., K. Seefeld, L. A. Witters, and R. A. Coleman. 1999. AMP-activated kinase reciprocally regulates triacylglycerol synthesis and fatty acid oxidation in liver and muscle: evidence that sn-glycerol-3-phosphate acyltransferase is a novel target. *Biochem. J.* **338:** 783–791.
18. Vila, M. C., G. Milligan, M. L. Standaert, and R. V. Farese. 1990. In-

sulin activates glycerol-3-phosphate acyltransferase (de novo phosphatidic acid synthesis) through a phospholipid-derived mediator. Apparent involvement of Giα and activation of a phospholipase C. *Biochemistry.* **29:** 8735–8740.
19. Yet, S. F., S. Lee, Y. T. Hahm, and H. S. Sul. 1993. Expression and identification of p90 as the murine mitochondrial glycerol-3-phosphate acyltransferase. *Biochemistry.* **32:** 9486–9491.
20. Folch, J., M. Lees, and G. H. S. Stanley. 1957. A simple method for the isolation and purification of total lipides from animal tissues. *J. Biol. Chem.* **226:** 497–509.
21. Lewin, T. M., D. A. Granger, J-H. Kim, and R. A. Coleman. 2001. Regulation of mitochondrial sn-glycerol-3-phosphate acyltransferase activity: response to feeding status is unique in various rat tissues and is discordant with protein expression. *Arch. Biochem. Biophys.* **396:** 119–127.
22. Acheson, K. J., Y. Schutz, T. Bessard, K. Anantharaman, J. P. Flatt, and E. Jequier. 1988. Glycogen storage capacity and de novo lipogenesis during massive carbohydrate overfeeding in man. *Am. J. Clin. Nutr.* **48:** 240–247.
23. Zammit, V. A. 1996. Role of insulin in hepatic fatty acid partitioning: emerging concepts. *Biochem. J.* **314:** 1–14.
24. Delzenne, N., P. Ferre, M. Beylot, C. Daubioul, B. Declercq, F. Diraison, I. Dugail, F. Foufelle, M. Foretz, K. Mace, R. Reimer, G. Palmer, G. Rutter, J. Tavare, J. Van Loo, and H. Vidal. 2001. Study of the regulation by nutrients of the expression of genes involved in lipogenesis and obesity in humans and animals. *Nutr. Metab. Cariovasc. Dis.* **11(Suppl.):** 118–121.
25. Obeid, O. A., J. Powell-Tuck, and P. W. Emery. 2000. The postprandial rates of glycogen and lipid synthesis of lean and obese female Zucker rats. *Int. J. Obes. Relat. Metab. Disord.* **24:** 508–513.
26. Marques-Lopes, I., D. Ansorena, I. Astiasaran, L. Forga, and J. A. Martinez. 2001. Postprandial de novo lipogenesis and metabolic changes induced by a high-carbohydrate, low-fat meal in lean and overweight men. *Am. J. Clin. Nutr.* **73:** 253–261.
27. Munday, M. R., M. R. Milic, S. Takhar, M. J. Holness, and M. C. Sugden. 1991. The short-term regulation of hepatic acetyl-CoA carboxylase during starvation and re-feeding in the rat. *Biochem. J.* **280:** 733–737.
28. Hastings, I. M., and W. G. Hill. 1990. Analysis of lines of mice selected for fat content. 2. Correlated responses in the activities of enzymes involved in lipogenesis. *Genet. Res.* **55:** 55–61.
29. McGarry, J. D., and N. F. Brown. 1997. The mitochondrial carnitine palmitoyltransferase system. From concept to molecular analysis. *Eur. J. Biochem.* **244:** 1–14.
30. Ruderman, N. B., A. K. Saha, V. Vavvas, and L. A. Witters. 1999. Malonyl-CoA, fuel sensing, and insulin resistance. *Am. J. Physiol.* **276:** E1–E18.
31. van der Leij, F. R., A. M. Kram, B. Bartelds, H. Roelofsen, G. B. Smid, J. Takens, V. A. Zammit, and J. R. G. Kuipers. 1999. Cytological evidence that the C-terminus of carnitine palmitoyltransferase I is on the cytosolic face of the mitochondrial outer membrane. *Biochem. J.* **341:** 777–784.
32. Kerner, J., and C. Hoppel. 2000. Fatty acid import into mitochondria. *Biochim. Biophys. Acta.* **1486:** 1–17.
33. Gonzalez-Baro, M. R., D. A. Granger, and R. A. Coleman. 2001. Mitochondrial glycerol phosphate acyltransferase contains two transmembrane domains with the active site in the N-terminal domain facing the cytosol. *J. Biol. Chem.* **276:** 43182–43188.
34. Kannan, L., J. Knudsen, and C. A. Jolly. 2003. Aging and acyl-CoA binding protein alter mitochondrial glycerol-3-phosphate acyltransferase activity. *Biochim. Biophys. Acta.* **1631:** 12–16.
35. Lee, Y., H. Hirose, Y. T. Zhou, V. Esser, J. D. McGarry, and R. H. Unger. 1997. Increased lipogenic capacity of the islets of obese rats: a role in the pathogenesis of NIDDM. *Diabetes.* **46:** 408–413.
36. Dircks, L. K., J. Ke, and H. S. Sul. 1999. A conserved seven amino acid stretch important for murine mitochondrial glycerol-3-phosphate acyltransferase activity. Significance of arginine 318 in catalysis. *J. Biol. Chem.* **274:** 34728–34734.